Fast and novel microseismic detection using time-frequency analysis

S.Mostafa Mousavi, and Charles A. Langston, University of Memphis*

Summary

An automatic algorithm for fast and robust detection of microseismic events recorded on surface arrays is presented based upon incorporating time-frequency thresholding and image processing techniques. To build a pseudo-characteristic function, time-frequency coefficients of the seismic trace are thresholded and resulting spectrums are transferred into histograms to detect high-energy arrivals associated seismic events. The main novelty of this methodology is incorporating a simple but powerful thresholding scheme that does not rely on any prior knowledge about noise level and an image processing step on the resulting spectrum that makes this method fast and adaptive. This approach is well suited for real time processing and detection of noisy microearthquakes.

Introduction

Robust detection of small microearthquakes especially using surface arrays is a challenging task due to typically high levels of background noise. The most common approaches that are currently used includecharacteristic-function (CF), cross-correlation (CC), and migration based methods. In CF-based methods, such as STA/LTA, abrupt changes in the time series are amplified using a characteristic function to automatically detect high amplitude signals. However, this method is known to be insensitive for detection of small amplitude microseismic events within high background noise and susceptible to false alarms. Although with a lower rate of false positives and more effective detection of low SNR events, CC-based methods such as match filtering (Gibbons and Ringdal 2006; Eisner et al. 2008) rely on availability of a high-SNR master (or template) event and are limited to event clusters with similar rupture mechanism and event signal. Migration-based detection performs relatively better (Cieplicki et al. 2014). It relies on obtaining a high value of the stack along the moveout curve computed from a hypothetical source position improving the SNR of the unstacked data (Duncan and Eisner 2010; Chambers et al., 2010, Gharti et al., 2010, Bradford et al., 2013). This method requires sufficient coherency in the arrival across the array and its success depends on polarity correction (Zhebel and Eisner 2012; Anikiev et al. 2013; Chambers et al. 2013). Moreover this method is sensitive to the noise level and existence of even one noisy trace in the stacking process can cause false positive (Thornton and Eisner, 2011).

In this study, high-energy arrivals in the time-frequency representation (TFR) of individual channels are used for event detection. SNR can be improved using time-frequency thresholding techniques, as well. However, these methods are usually computationally more expensive and not suited for real-time processing. We propose a simple and fast thresholding method based on general cross validation in the wavelet domain to amplify energy associated with seismic events in the TFR. The attenuated spectrum is further processed using image-processing techniques to build histograms that can be used for triggering and event detection. This approach is fast and automatic, hence holds great promise for real-time processing of single channel data with high noise level.

Theory and Method

The recorded signal y(t), can be represented by a sum of seismic signal components s_k, plus some additive noise $\varepsilon(t)$:

$$y(t) = \sum_{k=1}^{K} s_k(t) + \sigma\varepsilon(t) \tag{1}$$

where, K is the maximum number of components in the recorded signal and σ is the noise level.

The continuous wavelet transform (CWT) is a common transform used for time-frequency analyses. CWT is accomplished through a prototype analyzing function known as the mother wavelet ψ , which can be interpreted as a bandpass. The CWT of observed signal y , at scale a and time shift τ is given by (Daubechies, 1992):

$$W_y(a,\tau) = \langle y, \psi_{a,\tau} \rangle = \int_{-\infty}^{+\infty} y(t) a^{-1/2} \psi^*(\frac{t-\tau}{a}) dt \tag{2}$$

where , * denotes complex conjugate, $\langle y,\psi \rangle$ is the inner product, and W_y is the coefficient representing finite energy of the signal y in a concentrated time–frequency picture. The inversion of the CWT can be expressed as:

$$y(t) = \frac{1}{C_\psi} \int_a \int_\tau W_y(a,\tau) d\tau \frac{da}{a^2} \quad , \tag{3}$$

where the constant C_ψ is given by:

$$C_{\psi} = \int_{0}^{\infty} \xi^{-1} \hat{\psi}^{*}(\xi) d\xi \quad (4)$$

The CWT can be thought of as the cross–correlation of y with a number of wavelets that are stretched (or compressed) and shifted versions of the original mother wavelet ψ, such that oscillatory features across different frequencies are captured. The variable length of ψ leads to a flexible trade-off between time and frequency localization compared to the short time Fourier transfer (STFT). However, it still displays spectral smearing due to the finite size of the operator (Hall, 2006).

After transferring the observed data y into the CWT domain (using equation 2), SNR can be improved by attenuating the wavelet coefficients associated with the noise. Recalling the model in (1) for the recorded data (observation) y, the goal of signal enhancement is to remove as much of the additive noise ε as possible to improve the SNR. This can be achieved by an attenuation operator D that maps wavelet coefficients of noisy observations W_y, onto coefficients associated with an estimate of the signal of interest $W_{\tilde{s}} = D(W_y)$. A common choice for D is the soft-thresholding function of Donoho and Johnstone (1994) given by:

$$D(W_y) = \operatorname{sgn}(W_y) \ (|W_y| - \lambda)_+ \quad (5)$$

where sgn(.) is the sign function, $(.)_+$ indicates positive values, and λ is a threshold level.

The noise power can be suppressed by selecting a suitable threshold level λ. Wavelet coefficients in each scale are then thresholded using (5). The optimal threshold level λ *, is automatically determined for each decomposition level using the general cross validation (GCV) approach, proposed and developed by Nason (1994), and Weyrich and Warhola (1995). Following Jansen et al., (1997) the GCV function is defined as:

$$GCV(\lambda) = \frac{1/N \left\| T_y - \tilde{T}_{\lambda} \right\|^2}{\left(\frac{N_0}{N} \right)^2} \quad (6)$$

where, the $\tilde{T}_{\lambda}$ are thresholded coefficients using a threshold value of λ, and N_0 / N is the number fraction of coefficients that would be replaced by zero using this threshold level. This GCV is only a function of threshold value λ, and does not rely on noise level estimation. A grid search or minimization procedure such as the Fibonacci search then can be used to find the optimal threshold λ * producing a minimum GCV. Thresholding in this manner provides a fast and effective way to improve SNR of the TFR and to obtain the denoised signal using the inverse transform in (3).

The thresholded coefficients and resulting spectrum can then be used for further amplifying the high-energy arrivals and detection of microearthquakes using image-processing techniques. In this section we treat the spectrum as an image and instead of processing complex wavelet coefficients we work with pixels. This saves computational time and improves efficiency. Processing includes transforming the image into a binary version, color detection using Hue, transforming into a gray version, removing small specks, and transforming the gray image into a shaped histogram respectively. This histogram which contains the shapes and intensity of high-energy regions in the spectrum is easily used for event detection.

Synthetic Example

To test the thresholding method, a local synthetic seismogram and its contaminated version with random and real seismic noise (Figure 1b) with a SNR of 2.5 is used. Result of thresholding is presented in Figure 1c. In our implementation of the CWT, we use a Morlet wavelet.

The method was successful in removing the noise and improving the SNR; SNR was increased to 8. P and S energies are well preserved. However, some coda energy is attenuated. Denoised and synthetic signals match well over the entire waveform (Figure 1a and c) except at the very beginning of the P arrival and end of the P coda. Root-mean- squared error between denoised and synthetic signal is 0.046. Polarity and amplitude of the first two cycles of the P arrival are preserved very well. Cross-correlating the denoised signal with the synthetic one results in a maximum correlation coefficient of 0.82. Computation time is 0.9 sec that when compared to other thresholding methods (e.g. 39 sec for custom thresholding of Mousavi et al, submitted to Geophysics, 2015) is much lower and closer to the computational time of a simple band-pass filter (0.2 sec).

Field Example

We have applied the algorithm to real seismic data including microseismic events induced during wastewater

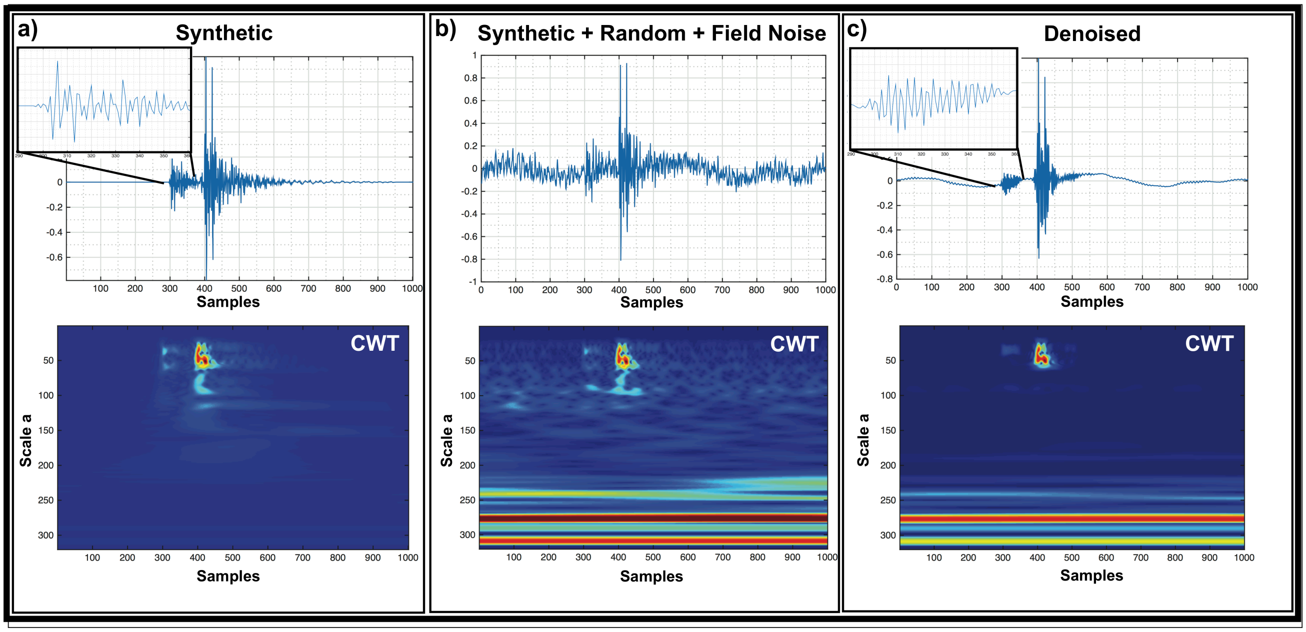

Figure 1: Synthetic test. a) synthetic signal and a zoomed window around P wave, b) contaminated with random and field noise, and c) after thresholding.

injection in central Arkansas, 2011, recorded by a broadband seismometer at the surface (Figure 2).

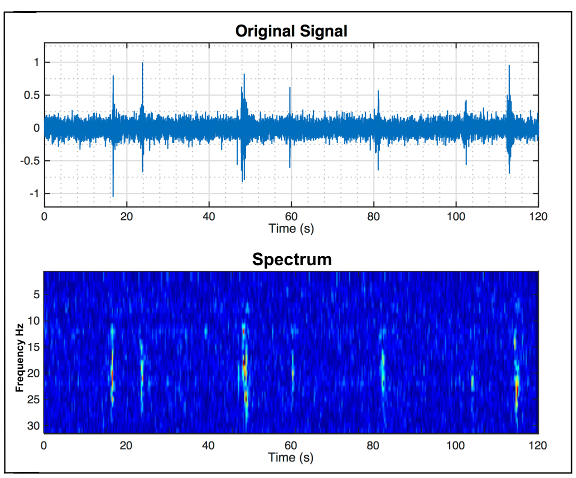

Figure 2: Top time series data of two minuets record of microroearthquakes induced by wastewater injection and bottom the wavelet spectrum.

The algorithm was successful in removing the noise and significantly improving the SNR (Figure 3). All seven events were preserved after thresholding. In the zoomed spectrum in Figure 4a, it can be seen clearly that six events out of seven were represented by high-power coefficients and one with relatively lower energy. To detect events, the thresholded spectrum is transform into a binary image and then into gray scale (Figure 4b). Pixels in this gray image can then be thresholded to pass pixels associated with events of high energy. This is equivalent to passing a triggering level in a normal detection algorithm. In the final step the threholded gray image is converted into histograms that indicate the number of microearthquakes and their relative magnitudes (Figure 4c).

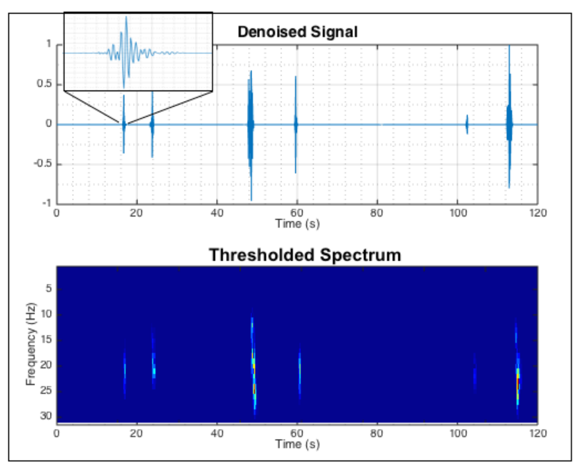

Figure 3: Top - time series of the denoised seismogram after thresholding and inverse transform. The bottom panel shows the thresholded wavelet spectrum.

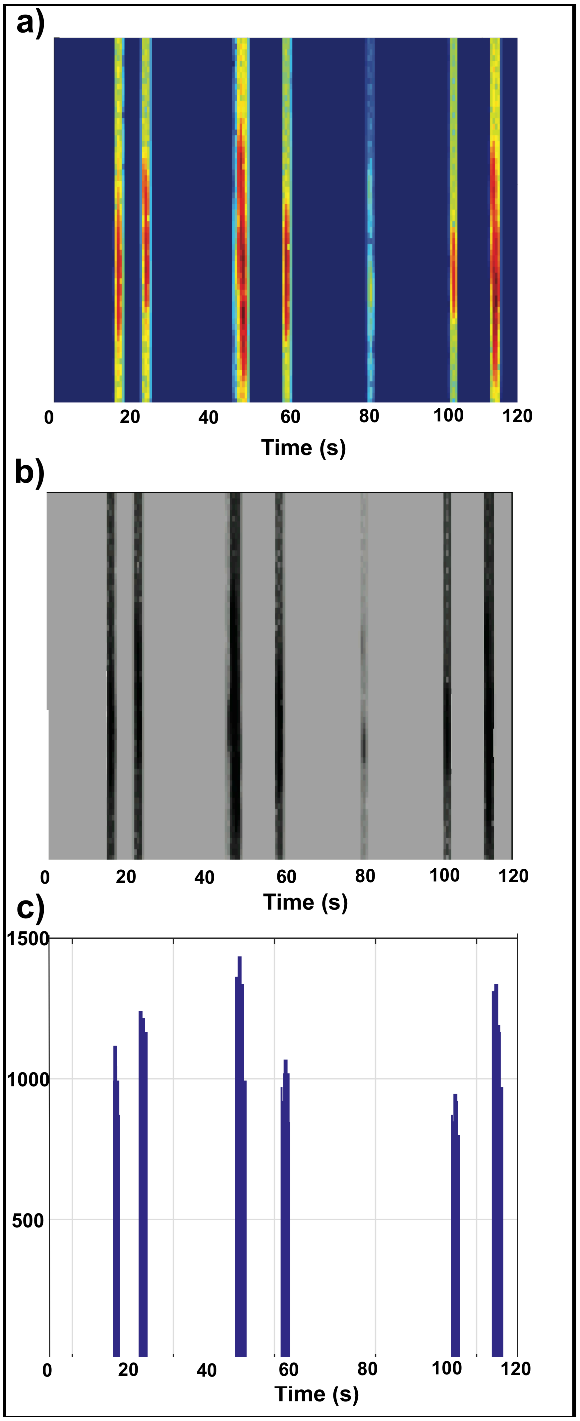

Figure 4: From top to bottom - thresholded spectrum, gray version, and histogram, respectively

Conclusion

A fast and adaptive algorithm is proposed for signal enhancement and detection of microseismic events using single channel data. This method incorporates time-frequency thresholding using the general cross validation technique and several image processing steps. The proposed method has been applied to both synthetic and field seismic data.

Simultaneous denoising and detection is shown to be important for increasing the accuracy of onset detection and efficiency in event detection. Because of the inherent crosscorrelation characteristic of the CWT, the proposed method can be compared with the denoising method of Eisner et al. (2008). In matched filtering (also known as the master-slave method) one event with high SNR is selected as the master event, a very narrow window around the peak amplitude is zero-lag crosscorrelated with the continuous waveform, and then the crosscorrelation coefficient traces from different stations are stacked to increase the SNR. The success of this method is based on the inherent ability of crosscorrelation in matching similar events and automatic removal of the move outs between the resulting coefficient traces. However the selection of one master event is the limiting factor in the process, which limits the efficiency of the method to similar events with close hypocenters and similar mechanisms. In our CWT-based method a mother wavelet with high correlation with the maximum energy of one event (equivalent to the master event) is selected, and is used in the cross correlation with the continuous record. The flexibility of the method is increased by the scaling procedure of the mother wavelet. This flexibility can be further improved by a more complicated automatic selection of the appropriate mother wavelet based on the nature of the dataset or using part of a master event's signal as the mother wavelet. This can simulate the use of secondary master events, or cousin events, in cross-correlation-based detection methods.

Acknowledgements

We thank Paul Ogwari for providing microseismic data. This research was supported by the Center for Earthquake Research and Information, University of Memphis

EDITED REFERENCES

Note: This reference list is a copyedited version of the reference list submitted by the author. Reference lists for the 2016 SEG Technical Program Expanded Abstracts have been copyedited so that references provided with the online metadata for each paper will achieve a high degree of linking to cited sources that appear on the Web.

REFERENCES

Anikiev, D., F. Stanek, J. Valenta, and L. Eisner, 2013, Imaging microseismic events by diffraction stacking with moment tensor inversion: SEG Technical Program Expanded Abstracts, **2013**, 2013–2018, http://dx.doi.org/10.1190/segam2013-0830.1.

Bradford, I., T. Probert, D. Raymer, A. Ozbek, P. Primiero, E. Kragh, J. Drew, and C. Woerpel, 2013, Application of Coalescence Microseismic Mapping to Hydraulic Fracture Monitoring Conducted Using a Surface Array: 75th EAGE Conference and Exhibition, http://dx.doi.org/10.3997/2214-4609.20131028.

Chambers, K., J. Clarke, R. Velasco, and B. Dando, 2013, Surface Array Moment Tensor Microseismic Imaging: 75th EAGE Conference and Exhibition, http://dx.doi.org/10.3997/2214-4609.20130404.

Chambers, K., J. M. Kendall, S. Brandsberg-Dahl, and J. Rueda, 2010, Testing the ability of surface arrays to monitor microseismic activity: Geophysical Prospecting, **58**, no. 5, 821–830, http://dx.doi.org/10.1111/j.1365-2478.2010.00893.x.

Cieplicki, R., L. Eisner, and M. Mueller, 2014, Microseismic event detection: comparing P-wave migration with P- and S-wave crosscorrelation: SEG Technical Program Expanded Abstracts, **2014**, 2168–2172, http://dx.doi.org/10.1190/segam2014-1614.1.

Daubechies, I., 1992, Ten Lectures on Wavelets, CBMS-NSF Regional Conference Series in Applied Mathematics, vol. 61, Society for Industrial and Applied Mathematics.

Donoho, D., and I. M. Johnstone, 1994, Ideal spatial adaptation by wavelet shrinkage: Biometrika, **81**, no. 3, 425–455, http://dx.doi.org/10.1093/biomet/81.3.425.

Duncan, P. and L. Eisner, 2010, Reservoir characterization using surface microseismic monitoring: Geophysics, **75**, no 5, 75A139–75A146, http://dx.doi.org/10.1190/1.3467760.

Eisner, L., D. Abbott, W. Barker, J. Lakings, and M. Thornton, 2008, Noise Suppression for Detection and Location of Microseismic Events Using a Matched Filter: 78th Annual International Meeting, SEG, Expanded Abstracts, 1431–1435.

Gharti, H., V. Oye, M. Roth, and D. Kühn, 2010, Automated microearthquake location using envelope stacking and robust global optimization: Geophysics, **75**, no. 4, MA27–MA46, http://dx.doi.org/10.1190/1.3432784.

Gibbons, S., and F. Ringdal, 2006, The detection of low magnitude seismic events using array-based waveform correlation: Geophysical Journal International, **165**, no. 1, 149–166, http://dx.doi.org/10.1111/j.1365-246X.2006.02865.x.

Hall, M., 2006, Resolution and uncertainty in spectral decomposition: First Break, **24**, no. 1102, 43–47, http://dx.doi.org/10.3997/1365-2397.2006027.

Jansen, M., M. Malfait, and A. Bultheel, 1997, Generalized cross validation for wavelet thresholding: Signal Processing, **56**, no. 1, 33–44, http://dx.doi.org/10.1016/S0165-1684(97)83621-3.

Nason, G. P., 1994, Wavelet regression by cross validation: University of Bristol.

Thornton, M., and L. Eisner, 2011, Uncertainty in surface microseismic monitoring: SEG Technical Program Expanded Abstracts, **2011**, 1524–1528, http://dx.doi.org/10.1190/1.3627492.

Weyrich, N., and G. T. Warhola, 1995, De-noising using wavelets and cross validation, S.P. Singh, ed., Approximation Theory: Wavelets and Applications, NATO Series C, 454, 523-532.

Zhebel, O., and L. Eisner, 2012, Simultaneous microseismic event localization and source mechanism determination: SEG Technical Program Expanded Abstracts, **2012**, 1–5, http://dx.doi.org/10.1190/segam2012-1033.1.